

DESIGN AND IMPLEMENTATION OF STRIPLINE FEEDBACK KICKERS IN THE MAX IV 3 GeV STORAGE RING

D. Olsson*, L. Malmgren, K. Åhnberg
MAX IV Laboratory, Lund, Sweden

Abstract

Commissioning of the Bunch-By-Bunch (BBB) feedback system in the MAX IV 3 GeV storage ring was started in early 2016. At the moment, the actuators are two stripline kickers oriented in the horizontal and in the vertical plane, respectively. Apart from providing feedback in the transverse plane, they are simultaneously operating as longitudinal actuators. This is done by upconverting the longitudinal 0 - 50 MHz baseband signal to the 150 MHz - 250 MHz range where the longitudinal shunt impedance of the striplines is higher. The upconverted signal is then fed to the stripline electrodes in common-mode. The design of the stripline kickers and the layout of the BBB feedback system in the 3 GeV ring are presented in this report. Results from instability studies in this ring are also discussed.

INTRODUCTION

The MAX IV facility in Lund, Sweden consists of two storage rings for production of synchrotron radiation, and a Short-Pulse-Facility (SPF) [1]. The two rings are designed for 3 GeV and 1.5 GeV, respectively, where the initial beam commissioning of the former has recently been completed, and commissioning of the latter was started in September 2016. Both rings will be operating with top-up injections delivered by a full-energy injector [2].

The two rings have been equipped with BBB feedback systems, where the signal processors are delivered by Dimtel [3]. In the 3 GeV ring, two stripline kickers that are dedicated for BBB feedback have been installed and commissioned. Apart from applying transverse feedback, the striplines are also simultaneously operating as weak longitudinal actuators and applying feedback in that plane too. The commission of the BBB feedback system in the 1.5 GeV has not yet been started.

The 3 GeV ring has been delivering synchrotron light to users since November 2016, and it has been observed that both longitudinal and transverse Coupled-Bunch-Mode-Instabilities (CBMIs) have a degrading effect on the quality of the light if they are not suppressed.

STRIPLINE DESIGN

The feedback stripline design is based on the diagnostic stripline used for tune measurements [4], and the cross-section and the dimensions of the geometry can be seen in Figure 1 and in Table 1, respectively. The main difference to the design in [4] is that the feedback striplines only have two electrodes, each with a length of $L = 300$ mm

(feedthrough-to-feedthrough). Each electrode has also two tapered sections of $L_t = 25$ mm. The tapered sections reduce the impedance mismatch between the electrodes and the coaxial feedthroughs, but they also suppress the beam impedance at higher frequencies as shown in [5]. The tapered sections can be seen in Figure 2. Both the vacuum chamber and the electrodes are made of stainless steel. The electrodes are welded to the inner conductors of the coaxial feedthroughs.

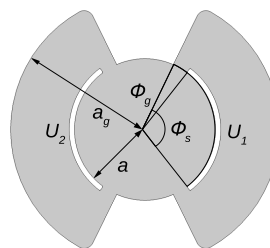


Figure 1: A transverse cross-section of the geometry.

Table 1: Parameters of the stripline geometry.

Parameter	
a	13.5 mm
a_g	25.2 mm
L	300 mm
L_t	25 mm
ϕ_s	107.20°
ϕ_g	12.75°

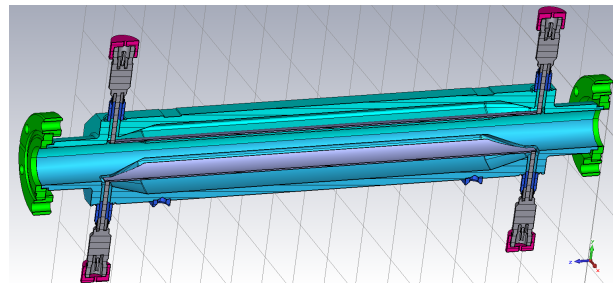


Figure 2: A cut-through of the stripline.

One can analytically obtain the electric scalar potential $\Phi(\rho, \phi)$ in the region $0 \leq \rho \leq a$ of the first propagating TEM modes by solving Laplace equation in 2D by using the methods presented in [6]. $\Phi(\rho, \phi)$ is given by (1), and the electric field is then obtained as $\mathbf{E}(\rho, \phi) = -\nabla\Phi(\rho, \phi)$. Here we assume that the electric field in the four gaps between the electrodes and the zero-potential chamber walls at $\rho = a$ is constant and purely azimuthal, thus $\mathbf{E}(a, \phi) = \pm \frac{U_1}{a\phi_g} \hat{\phi}$. The potential of the two electrodes (see Figure 1) for the odd and even mode are $U_1 = -U_2$ and $U_1 = U_2$, respectively. The odd mode is excited when driving the stripline in differential-mode and applying transverse feedback, while the even mode is excited when driving the stripline in common-mode and applying longitudinal feedback. Figure 3 shows $\Phi(\rho, \phi)$ ob-

* email: david.olsson@maxiv.lu.se

$$\Phi(\rho, \phi) = \frac{\phi_g + \phi_s}{2\pi} (U_1 + U_2) + \frac{4}{\pi\phi_g} \sum_{n=1}^{\infty} \left(\frac{\rho}{a}\right)^n \frac{\sin\left(n\frac{\phi_g}{2}\right) \sin\left(n\frac{\phi_s + \phi_g}{2}\right)}{n^2} (U_1 \cos(n\phi) + U_2 \cos(n(\phi - \pi))) \quad (1)$$

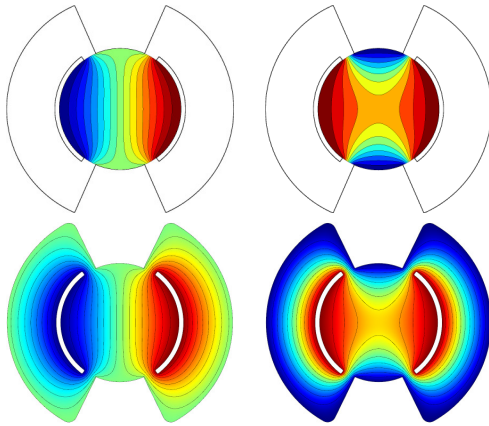


Figure 3: $\Phi(\rho, \phi)$ obtained analytically from (1) (upper), and numerically from COMSOL (lower). The left figures show the odd mode, and the right ones show the even mode.

tained from (1) and from electrostatic simulations in COMSOL Multiphysics [7].

The width of the two electrodes ϕ_s are optimized for on-axis field homogeneity when operating in differential mode, and a_g is set to obtain a characteristic impedance close to 50 Ω . The characteristic impedance of a single electrode when operating in differential and common-mode are $Z_{0,\perp} = 47.2 \Omega$ and $Z_{0,\parallel} = 52.9 \Omega$, respectively, and they are chosen so that $\sqrt{Z_{0,\perp}Z_{0,\parallel}} = 50 \Omega$. The transverse and longitudinal shunt impedances, $R_{\perp}(\omega)$ and $R_{\parallel}(\omega)$, of a stripline can be approximated as

$$R_{\perp}(\omega) = 2Z_{0,\perp} \left(\frac{g_{\perp}c_0}{a}\right)^2 \frac{\sin^2\left(\frac{\omega(L-L_t)}{c_0}\right) \sin^2\left(\frac{\omega L_t}{c_0}\right)}{\omega^2 \left(\frac{\omega L_t}{c_0}\right)^2} \quad (2)$$

$$R_{\parallel}(\omega) = 2Z_{0,\parallel} g_{\parallel}^2 \sin^2\left(\frac{\omega(L-L_t)}{c_0}\right) \frac{\sin^2\left(\frac{\omega L_t}{c_0}\right)}{\left(\frac{\omega L_t}{c_0}\right)^2} \quad (3)$$

where $g_{\perp} = a|\mathbf{E}(\rho=0)|/U_1 = 1.10$ and $g_{\parallel} = \Phi(\rho=0)/U_1 = 0.67$ are the transverse and longitudinal geometry factors obtained for the odd and even mode, respectively as defined in [8]. $R_{\perp}(\omega)$ and $R_{\parallel}(\omega)$ obtained analytically and from frequency domain simulations in COMSOL are shown in Figure 4.

Figure 5 - 6 show the differential (S_{ddx1}) and common mode (S_{ccx1}) S-parameters, respectively obtained from COMSOL and from measurements with a 4-port vector network analyser. In the mixed-mode measurements, the two physical downstream ports form the first logical port, while the two physical upstream ports form the second logical port.

ISBN 978-3-95450-182-3

4286

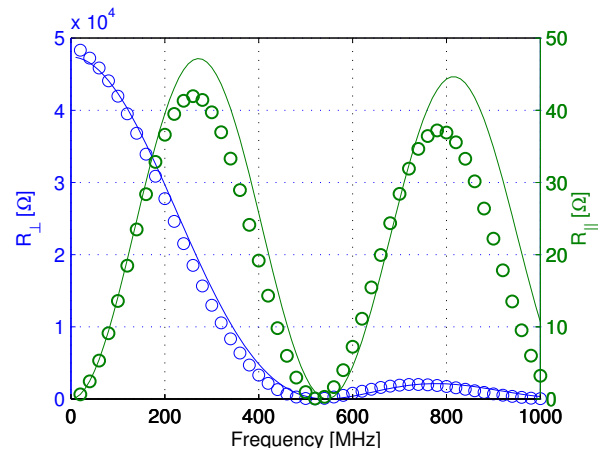


Figure 4: $R_{\perp}(\omega)$ and $R_{\parallel}(\omega)$ obtained from (2)-(3) (solid lines) and from COMSOL (circles).

The dominant source for impedance mismatch and transmission losses are the ceramic feedthroughs. Note that three narrow-band notches are visible in the measured data above 4 GHz in Figure 5 but not in Figure 6. These are eigenmodes with dipole components (hence only excited in differential mode) that are trapped inside the structure.

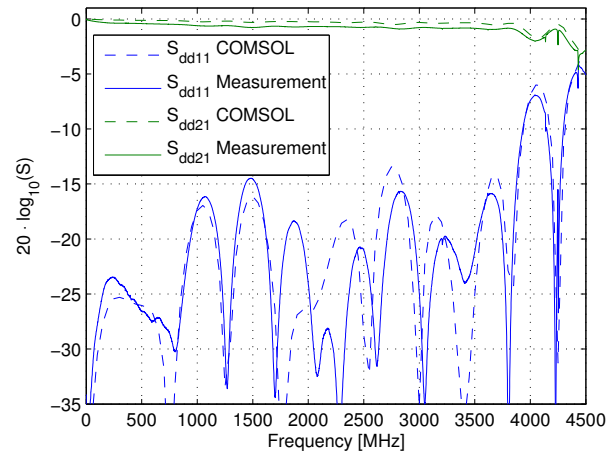


Figure 5: The measured and simulated differential-mode S-parameters.

The main ring RF system in MAX IV is operating at 100 MHz [9], so the span of the BBB feedback baseband signals is 0-50 MHz. Both striplines are simultaneously operating as weak longitudinal actuators. This is possible by feeding the longitudinal baseband signal, upconverted to the 150 MHz-250 MHz range, in common-mode to the electrodes. As seen

07 Accelerator Technology

T06 Room Temperature RF

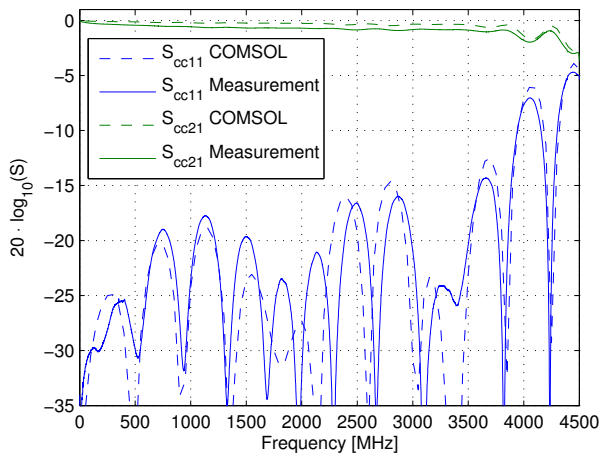


Figure 6: The measured and simulated common-mode S-parameters.

in Figure 4, $R_{||}(\omega)$ is quite low, and an overloaded cavity that will operate as a permanent longitudinal actuator is being constructed, and it will be installed in June 2017 [10]. Figure 7 shows a simplified circuit diagram of the upconverting back-end, where BB(x/y/z)(+/-) are the differential-mode baseband signals from the signal processors. The four output signals are fed to the four stripline electrodres via broad-band R&S BBA150 drive amplifiers [11].

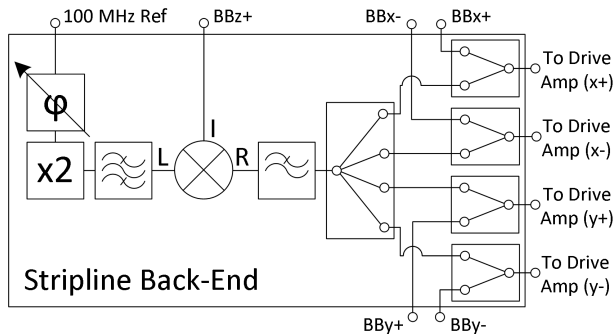


Figure 7: A simplified circuit diagram of the stripline back-end.

COUPLED-BUNCH INSTABILITIES IN THE 3 GeV RING

The longitudinal CBMIs in the 3 GeV ring are driven by Higher-Order Modes (HOMs) in the main and in the 3:rd harmonic (Landau) cavities, and it has been possible to suppress them with feedback at currents well above 100 mA this far even with the Landau cavities completely detuned (without any bunch lengthening). This was, however, only possible after mapping the dangerous HOMs in the cavities and by tuning their resonance frequencies away from the frequencies of the nearby coupled-bunch modes that are

driving the instabilities. Figure 8 shows the longitudinal bunch profile measured with a sampling oscilloscope at the diagnostic beamline [12] with longitudinal feedback ON and OFF. The Landau cavities are here detuned, so the profile of the stable bunch is rather Gaussian. The much wider profile observed without feedback is mainly due to longitudinal dipole oscillations of the bunches and due to the fact that the sampling oscilloscope is unable to capture data from a single bunch at a single turn. The centroid of the unstable bunches are here oscillating with a magnitude of approximately ± 200 ps which corresponds to $\pm 7.2^\circ$ relative to the 100 MHz RF system.

The observed CBMIs in the transverse plane have this far mainly been driven by ions, and the threshold where they appear has moved towards higher beam currents as the quality of the vacuum has improved. The transverse feedback voltage provided by the striplines has this far been more than enough to suppress them.

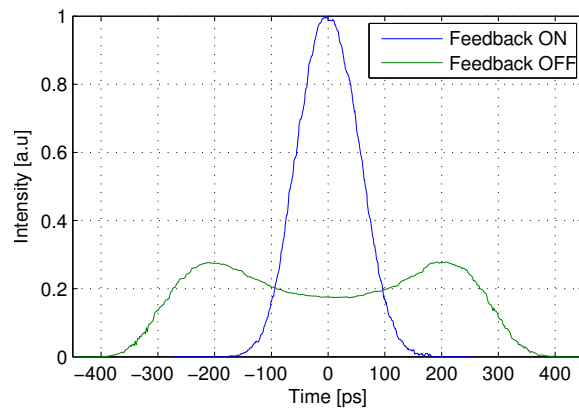


Figure 8: The longitudinal bunch profile measured at the diagnostic beamline at a beam current of 70 mA.

CONCLUSIONS AND FUTURE WORK

This far, the BBB feedback system has been able to suppress the transverse and longitudinal CBMIs in the 3 GeV ring at currents above 100 mA, and it has made it possible to deliver a stable beam to the first users at MAX IV. More powerful feedback can soon be applied in the longitudinal plane when the overloaded cavity is installed during the summer of 2017. Commissioning of the BBB feedback system in the 1.5 GeV ring will be carried out in the second half of 2017.

ACKNOWLEDGEMENTS

The authors would like to thank Åke Andersson, Francis Cullinan, Pedro Fernandes Tavares, and Jens Sundberg for their help during the measurements and during the commissioning of the BBB feedback system. Also big thanks to Dmitry Teytelman at Dimtel for all the support.

REFERENCES

- [1] P. F. Tavares *et al.*, “The MAX IV storage ring project”, *Jour. of Synch. Rad.*, 21, pp. 862–877, 2014.
- [2] S. Thorin *et al.*, “The MAX IV LINAC”, in *Proc. 27:th Linear Acc. Conf. (LINAC’14)*, Geneva, Switzerland, Sep. 2014, paper TUIOA03, pp. 400–403.
- [3] Dimtel, <http://www.dimtel.com/>.
- [4] D. Olsson, “Design of Stripline Kicker for Tune Measurements in the MAX IV 3 GeV Ring”, in *Proc. 34:th Progress in Electromagnetic Research Symp. (PIERS’13)*, Stockholm, Sweden, Aug. 2013, pp. 1095–1099.
- [5] C. Belver-Aguilar *et al.*, “Stripline design for the extraction kicker of Compact Linear Collider damping rings”, *Phys. Rev. ST Acc. Beams*, 17, 071003, 2010.
- [6] J. D. Jackson, in *Classical Electrodynamics Third Edition*, Chapter 2-3, John Wiley & Sons, 1998.
- [7] COMSOL Multiphysics, <http://www.comsol.com/>.
- [8] D. A. Goldberg and G. R. Lambertson, “Dynamic Devices A Primer on Pickups and Kickers”, in *AIP Conf. Proc. Series - Phys. of Part. Acc.*, 1992.
- [9] Å. Andersson *et al.*, “The 100 MHz RF system for the MAX IV storage rings”, in *Proc. 2:nd Int. Part. Acc. Conf. (IPAC’11)*, San Sebastian, Spain, Sep. 2011, paper MOPC05, pp. 193–195.
- [10] D. Olsson *et al.*, “A Waveguide Overloaded Cavity Kicker for the MAX IV Bunch-by-Bunch Feedback System”, in *Proc. 8:th Int. Part. Acc. Conf. (IPAC’17)*, Copenhagen, Denmark, May. 2017, paper THPIK087.
- [11] Rohde & Schwarz, <http://www.rohde-schwarz.com>.
- [12] J. Breunlin *et al.*, “Emittance diagnostics at the MAX IV 3 GeV storage ring”, in *Proc. 7:th Int. Part. Acc. Conf. (IPAC’16)*, Busan, Korea, May. 2016, paper WEPOW034, pp. 2908–2910.